Light scattering properties of paramagnetic particles

Y.-B. Du and P. Tong
Department of Physics, Oklahoma State University, Stillwater, Oklahoma 74078

(Received 24 February 1997; accepted 2 April 1997)

We present an experimental study of light scattering properties of paramagnetic particles. To account for the magnetic dipole radiation and the Brownian motion of the particles in a thermal equilibrium solution, we calculate the scattering intensity and its auto-correlation function $g(t)$. Experimentally, we examine the scattering properties of the paramagnetic particles and compare the results with those from isotropic and anisotropic dielectric particles. The experiment verifies the calculation and reveals that the magnetic dipole radiation of the paramagnetic particles is unusually large and equals to approximately 1/3 of the electric dipole radiation of the particles. Dynamic light scattering measurements show that the measured $g(t)$ for the depolarized scattering is strongly influenced by the size distribution of the particles. This is because the large paramagnetic particles tend to have more magnetite content and hence weigh more in the depolarized scattering. With a simple sedimentation method, we are able to separate the particles of different sizes and obtain relatively monodispersed scattering samples. These samples give the expected translational and rotational diffusion constants of the particles.
[S0021-9606(97)01026-X]

I. INTRODUCTION

In recent years there has been a growing interest in studying the structure and phase behavior of suspensions of paramagnetic particles and droplets.[1–6] These particles are polymer latex spheres (or oil droplets) which contain many tiny crystallites of magnetite (Fe_3O_4) or maghemite (γ-Fe_2O_3). Because of the random orientation of the ferrimagnetic crystallites, which are uniformly dispersed in the latex spheres,[7] the net magnetic dipole moment of the particles is zero when an external magnetic field is absent. Under this condition, the particles behave like hard spheres in a thermal equilibrium solution. When an external magnetic field is applied to the paramagnetic suspension, the particles interact through the induced magnetic dipole moments and they can form an array of particle chains parallel to the direction of the external field. Because of the complicated dipolar as well as thermal and hydrodynamic interactions between the particles, the paramagnetic suspensions exhibit rich phase behavior and dynamics. Laser light scattering and other experimental methods have been used to study the structure and dynamics in these systems.[6,8–10] In the previous light scattering experiments, the paramagnetic particles were treated as simple dielectric spheres and no attempt was made to study how the induced magnetic dipole moment of these particles affects their scattering properties.

In this paper we present an experimental study of light scattering properties of the paramagnetic particles. To account for the magnetic dipole radiation and the Brownian motion of the particles in a thermal equilibrium solution, we calculate the scattering intensity and its auto-correlation function $g(t)$. The calculation clearly delineates the difference in the scattering property between the dielectric and paramagnetic particles. Experimentally, we examine the scattering properties of the paramagnetic particles and compare the results with those from isotropic and anisotropic dielectric particles. The experiment verifies the calculation and reveals that the magnetic dipole radiation of the paramagnetic particles is unusually large and equals to approximately 1/3 of the electric dipole radiation of the particles. The magnetic dipole radiation is presumably resulted from the alignment of the individual ferrimagnetic grains, which are uniformly dispersed inside the particles, and that this alignment is induced by the incident laser light. Dynamic light scattering measurements show that the measured intensity auto-correlation function $g(t)$ for the depolarized scattering is strongly influenced by the size distribution of the particles. This is because the large paramagnetic particles tend to have more magnetite content and hence weigh more in the depolarized scattering. With a simple sedimentation method, we are able to separate the particles of different sizes and obtain relatively monodispersed scattering samples. These samples give the expected translational and rotational diffusion constants of the particles.

The paper is organized as follows. In Section II, we review the scattering theory for the magnetic dipole radiation and present the calculation of the electric field auto-correlation function for the small paramagnetic particles. Experimental details appear in Section III, and the results are discussed in Section IV. Finally, the work is summarized in Section V.

II. THEORY

The basic light scattering theory is well documented.[11,12] Here we reframe the theory so as to account for the magnetic dipole radiation and the Brownian motion of the paramagnetic particles in a thermal equilibrium solution. Figure 1 shows the schematic diagrams of the experimental setup and the scattering geometry. The scattering plane is defined by the incident wave vector $\mathbf{k}_i$ and the scattered wave vector

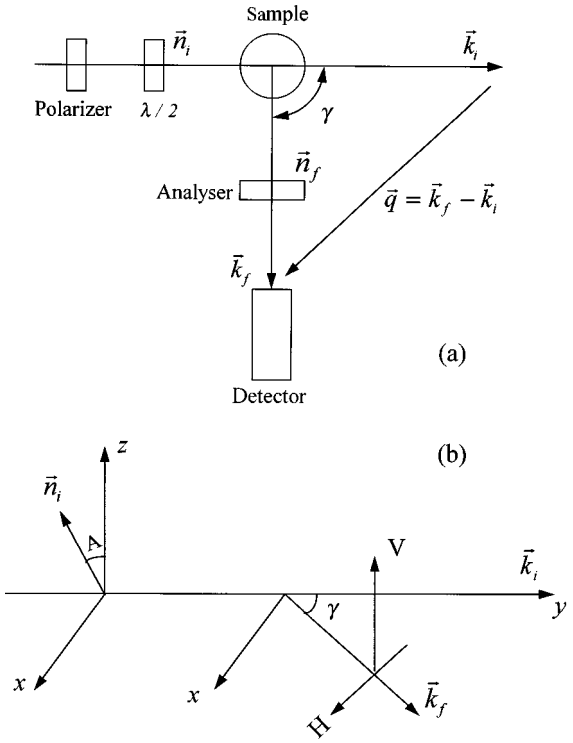

FIG. 1. (a) Schematic diagram of the experimental setup: $\mathbf{k}_i$, $\mathbf{k}_f$, incident and scattered wave vectors; $\mathbf{n}_i$, $\mathbf{n}_f$, polarization directions of the incident and detected light; γ, scattering angle. (b) Schematic diagram of the scattering geometry: **V** is perpendicular to the x-y plane; **H** is in the x-y plane and is perpendicular to $\mathbf{k}_f$; $\mathbf{n}_i$ is in the x-z plane having an angle A with respect to the z axis.

$\mathbf{k}_f$. The momentum transfer vector is given by $\mathbf{q}=\mathbf{k}_f-\mathbf{k}_i$, and its amplitude equals $q=(4\pi n/\lambda_0)\sin(\gamma/2)$. Here γ is the scattering angle, n is the refractive index of the solvent, and λ_0 is the wavelength of the incident light. The polarization direction $\mathbf{n}_i$ of the incident light is in the x-z plane and is specified by the angle A with respect to the z axis. The polarization direction $\mathbf{n}_f$ of the detected light can be either perpendicular to the scattering plane (the AV scattering geometry) or parallel to the scattering plane (the AH scattering geometry).

We now consider the scattering by N identical particles, whose molecular polarizability tensor is $\hat{\alpha}(t)$. The total scattered electric field, $\mathbf{E}_{i,f}(t)$, is a sum of the fields radiated by each of the particles in the illuminated volume, and has the form[12]

$$\mathbf{E}_{i,f}(t)=\sum_{j=1}^{N}\alpha_{i,f}^{j}(t)e^{-i\mathbf{q}\cdot\mathbf{r}_j(t)},\neg \tag{1}$$

where $\mathbf{r}_j(t)$ is the position of the center of mass of the jth particle at time t, and $\alpha_{i,f}(t)=\mathbf{n}_f\cdot\hat{\alpha}(t)\cdot\mathbf{n}_i$ is the component of $\hat{\alpha}(t)$ along the initial polarization direction $\mathbf{n}_i$ and the final polarization direction $\mathbf{n}_f$, both of them being fixed in the laboratory. For particles suspended in a thermal equilibrium solution, their rotational motion may cause $\alpha_{if}(t)$ to vary with time t. The phase factor $e^{-i\mathbf{q}\cdot\mathbf{r}(t)}$ changes with time because the particles move. The electric field auto-correlation function then becomes

$$\begin{aligned}I_{i,f}(q,t)&=\langle\mathbf{E}_{i,f}^{*}(t')\mathbf{E}_{i,f}(t'+t)\rangle\\&=\sum_{j,k}^{N}\langle\alpha_{i,f}^{j}(t')\alpha_{i,f}^{k}(t'+t)e^{-i\mathbf{q}\cdot[\mathbf{r}_j(t')-\mathbf{r}_k(t'+t)]}\rangle\\&=N\langle\alpha_{i,f}(t')\alpha_{i,f}(t'+t)\rangle F(q,t),\neg\end{aligned} \tag{2}$$

where the angular brackets represent a time average over t', and $F(q,t)=\langle\exp\{-i\mathbf{q}\cdot[\mathbf{r}_j(t')-\mathbf{r}_j(t'+t)]\}\rangle$ is the ''translational'' factor. To get the last equality in Eq. (2), we have made following assumptions. (1) There is no spatial and temporal correlations between different particles in a dilute solution, so that all the cross terms can be neglected. (2) The phase and amplitude fluctuations of the scattered electric field are statistically independent. These approximations are certainly valid for the Brownian motion of the particles in a dilute solution at thermal equilibrium. When the delay time $t=0$, $I_{i,f}(q,0)$ is simply the scattered light intensity.

A. Scattering in different incident polarization direction $\mathbf{n}_i$

We first calculate $I_{i,f}(q,t)$ for different $\mathbf{n}_i$ when the scattering angle γ is fixed at 90°. For the paramagnetic particles used in the experiment, both the electric dipole source and the magnetic dipole source contribute to the polarizability tensor $\hat{\alpha}(t)$. To account for the optical anisotropy, we assume that the electric and magnetic polarizability tensors of the particles are of cylindrical symmetry and can be simultaneously diagonalized in the molecular coordinate system x', y', z'. In this case, we have[11]

$$\begin{aligned}\alpha_{i,f}&=\mathbf{n}_f\cdot\hat{\alpha}_{\mathbf{e}}\cdot\mathbf{n}_i+\mu(\hat{\mathbf{k}}_f\times\mathbf{n}_f)\cdot\hat{\alpha}_{\mathbf{e}}\cdot(\hat{\mathbf{k}}_i\times\mathbf{n}_i)\\&=(\alpha_e)_{i,f}+\mu(\alpha_e)_{i+90°,f+90°},\neg\end{aligned} \tag{3}$$

where μ is the ratio of the particle's magnetic dipole moment to its electric counterpart, and $\hat{\mathbf{k}}_i$ and $\hat{\mathbf{k}}_f$ are, respectively, the incident and scattered wave vectors as shown in Fig. 1(a). The subscript $+90°$ indicates a 90°-rotation for the corresponding polarization vectors (anti-clockwise when facing to the wave vectors). This rotation can be understood by the fact that the electric and magnetic radiations are perpendicular with each other. To calculate $\langle\alpha_{i,f}(t')\alpha_{i,f}(t'+t)\rangle$ in Eq. (2), the laboratory-fixed component $\alpha_{if}(t)$ has to be expressed in terms of the molecular-fixed components. In the molecular coordinate system x', y', z', the electric polarizability tensor $\hat{\alpha}_e$ takes the form

$$\hat{\alpha}_e=\begin{pmatrix}\alpha_{\parallel}&0&0\\0&\alpha_{\perp}&0\\0&0&\alpha_{\perp}\end{pmatrix},\quad\neg \tag{4}$$

where $\alpha_{\parallel}$ is the polarizability component parallel to the symmetry axis of the particle and $\alpha_{\perp}$ is that in any direction perpendicular to this axis.

The projection of the unit vectors $\hat{\mathbf{x}}$, $\hat{\mathbf{y}}$, $\hat{\mathbf{z}}$ in the laboratory-fixed coordinate system along the x', y', z' axes of the molecular coordinate system gives[12]

$$\hat{\mathbf{x}}=\begin{pmatrix}\sin\theta\cos\phi\\ -\cos\theta\cos\phi\\ \sin\phi\end{pmatrix},$$

$$\hat{\mathbf{y}}=\begin{pmatrix}\sin\theta\sin\phi\\ -\cos\theta\sin\phi\\ -\cos\phi\end{pmatrix},$$

$$\hat{\mathbf{z}}=\begin{pmatrix}\cos\theta\\ \sin\theta\\ 0\end{pmatrix}.\neg \tag{5}$$

In the above, the spherical coordinates θ and ϕ specify the orientation of the particle's symmetry axis in the laboratory-fixed coordinate system. As shown in Fig. 1(b), the incident polarization direction $\mathbf{n}_i$ can be written as

$$\mathbf{n}_i=(\cos A)\hat{\mathbf{z}}+(\sin A)\hat{\mathbf{x}}.\neg \tag{6}$$

With Eqs. (4)–(6) one can calculate

$$\alpha_{A,Z}=(\alpha_e)_{A,Z}+\mu(\alpha_e)_{A+90^\circ,Z+90^\circ}$$
$$=(\alpha_e)_{A,Z}+\mu(\alpha_e)_{A+90^\circ,-Y} \tag{7}$$

for the AV scattering geometry and

$$\alpha_{A,-Y}=(\alpha_e)_{A,-Y}+\mu(\alpha_e)_{A+90^\circ,-Y+90^\circ}$$
$$=(\alpha_e)_{A,-Y}+\mu(\alpha_e)_{A+90^\circ,-Z} \tag{8}$$

for the AH scattering geometry. The final results are

$$I_{A,Z}(q,t)=N\left\{\left(\alpha^2+\frac{\beta^2}{45}e^{-6\Theta t}\right)\cos^2 A + \frac{\beta^2}{15}(1+\mu^2)e^{-6\Theta t}\right\}F(q,t) \tag{9}$$

and

$$I_{A,-Y}(q,t)=N\left\{\mu^2\left(\alpha^2+\frac{\beta^2}{45}e^{-6\Theta t}\right)\sin^2 A + \frac{\beta^2}{15}(1+\mu^2)e^{-6\Theta t}\right\}F(q,t).\neg \tag{10}$$

In the above, $\beta\equiv(\alpha_\parallel-\alpha_\perp)$, $\alpha\equiv(\alpha_\parallel+2\alpha_\perp)/3$, and Θ is the rotational diffusion constant of the particles. To get Eqs. (9) and (10), we have assumed that the particles are undergoing Brownian motion in a thermal equilibrium solution. In this case the ''translational'' factor is given by $F(q,t)=e^{-Dq^2t}$, with D being the translational diffusion constant. Both D and Θ have been calculated previously for spherical and rod-like particles.[12] For most optically anisotropic particles, their isotropic scattering ($\propto\alpha^2$) is usually much larger than the anisotropic scattering ($\propto\beta^2$).

From Eqs. (9) and (10) one can clearly see the difference in the scattering property between the dielectric and paramagnetic particles. For dielectric particles ($\mu=0$), their $I_{A,Z}(q,0)$ is dominated by the electric dipole contribution $N\alpha^2\cos^2 A$. If the particles possess optical anisotropy ($\beta\neq0$), their depolarized intensity $I_{A,-Y}(q,0)$ goes as $N\beta^2/15$, which does not change with the polarization angle A.¬ This small A-independent term also appears in $I_{A,Z}(q,0)$. For the paramagnetic particles ($\mu\neq0$), their $I_{A,Z}(q,0)$ is approximately the same as that of the dielectric particles, except the A-independent term is increased by a factor of $1+\mu^2$. However, their depolarized intensity $I_{A,-Y}(q,0)$ differs greatly from that of the dielectric particles and is dominated by the magnetic dipole contribution $N\mu\alpha^2\sin^2 A$. Because of the phase difference between $\sin^2 A$ and $\cos^2 A$, one can easily distinguish the electric and magnetic dipole radiations by changing the polarization angle A.

B. Scattering at different scattering angle γ

We now fix $\mathbf{n}_i$ to be vertical ($A=0^\circ$) and calculate $I_{i,f}(q,t)$ for different scattering angle γ. In this case, we have

$$\alpha_{Z,Z}=(\alpha_e)_{Z,Z}+\mu(\alpha_e)_{Z+90^\circ,Z+90^\circ}$$
$$=(\alpha_e)_{Z,Z}+\mu(\alpha_e)_{X,H} \tag{11}$$

for the VV scattering geometry and

$$\alpha_{Z,H}=(\alpha_e)_{Z,H}+\mu(\alpha_e)_{Z+90^\circ,H+90^\circ}$$
$$=(\alpha_e)_{Z,H}+\mu(\alpha_e)_{X,-Z} \tag{12}$$

for the VH scattering geometry. As shown in Fig. 1(b), the horizontal polarization direction $\mathbf{H}$ of the detected light takes the form

$$\mathbf{H}=(\cos\gamma)\hat{\mathbf{x}}-(\sin\gamma)\hat{\mathbf{y}}.\neg \tag{13}$$

With Eqs. (11)–(13) we find

$$I_{V,V}(q,t)=N\left\{\left(\alpha^2+\frac{\beta^2}{45}e^{-6\Theta t}\right)(1+\mu\cos\gamma)^2 + \frac{\beta^2}{15}e^{-6\Theta t}(1-2\mu\cos\gamma+\mu^2)\right\}F(q,t) \tag{14}$$

and

$$I_{V,H}(q,t)=N\frac{\beta^2}{15}e^{-6\Theta t}(1-2\mu\cos\gamma+\mu^2)F(q,t). \tag{15}$$

In the study of the structure and the particle interaction of concentrated colloidal suspensions, one usually measures the structure factor $S(q)$, which is the scattered intensity $I_{V,V}(q,0)$ normalized by the number of the particles in the scattering volume and their form factor. For suspensions of the paramagnetic particles (assuming $\beta=0$), however, one needs to further divide out an extra factor $(1+\mu\cos\gamma)^2$ in the measured $I_{V,V}(q,0)$ [see Eq. (14)], in order to obtain a correct form of $S(q)$. The effect of $(1+\mu\cos\gamma)^2$ is particularly large for the paramagnetic particles with large μ, and has not been considered in previous light scattering experi-

ments. To study the motion of the particles in the solution, one needs to examine the time dependence of the electric field auto-correlation function $I_{i,f}(q,t)$. Experimentally, $I_{i,f}(q,t)$ is obtained by measuring the intensity auto-correlation function

$$g(t)=\frac{\langle I_{i,f}(t')I_{i,f}(t'+t)\rangle}{\langle I_{i,f}(t')\rangle^2}=1+b\left\{\frac{I_{i,f}(q,t)}{I_{i,f}(q,0)}\right\}^2, \qquad (16)$$

where $b(\leqslant 1)$ is an instrumental constant which depends on the geometry of the experimental setup. To get the last equality in Eq. (16), we have used the fact that the scattered light from a thermal equilibrium solution obeys Gaussian statistics.[12] Measurements of $g(t)$ have been especially fruitful in studies of the translational and rotational diffusion of small particles.[12–15]

III. EXPERIMENT

The paramagnetic particles used in the experiment were purchased from Bangs Laboratories. These particles are polymer latex spheres which contain 67 wt.% magnetite (Fe_3O_4). The magnetite forms many tiny ferrimagnetic crystallites of size $\sim$5 nm, which are uniformly dispersed in the latex spheres.[7] Because of the random orientation of the ferrimagnetic crystallites, the latex spheres possess no net magnetization in zero magnetic field. The particles can be easily magnetized by a weak external magnetic field such as a bar magnet, and have been widely used in cell separation, protein purification, and DNA isolation, when their surfaces are coated with certain binding biomolecules. The surfaces of our particles were modified by the carboxylic acid functional groups and the electric charges associated with the functional groups stabilized the particles in an aqueous solution. The stock solution contained 10 wt.% solid particles, and the scattering samples were prepared by diluting known amounts of the concentrated suspension with distilled water. A small amount of sodium dodecyl sulfate (SDS) surfactant (0.5 wt.%) was added to the dilute solution in order to enhance the stability of the suspension. To eliminate particle aggregates, each sample was sonicated for several minutes prior to the scattering measurements.

Light scattering measurements were performed using a standard scattering goniometer. A schematic diagram of the experimental setup is shown in Fig. 1(a). The light source was a 30 mW He-Ne laser (Spectra Physics, Model 127). The sample cell was immersed in a toluene bath in order to match the refractive index of the glass cell and hence reduce the background scattering from the glass wall. The scattered light intensity from a well-defined scattering volume was recorded by an avalanche photodiode detector (EG&G, SPCM-100-PQ). Intensity measurements were accumulated for periods of 30–60 seconds. The incident polarization direction $\mathbf{n}_i$ was varied by rotating a $\lambda/2$ waveplate. The polarizers used in the experiment were Glan-Thompson calcite polarizing prisms, which were purchased from Mells Griot. An ALV-5000 multi-τ correlator was used to measure the intensity auto-correlation function $g(t)$. All the scattering measurements were made at room temperature.

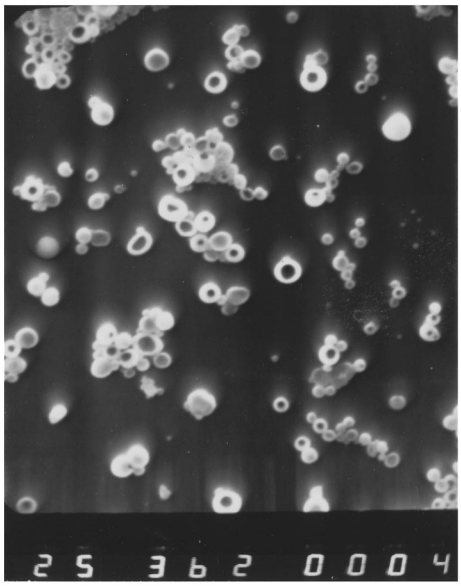

FIG. 2. Scanning electron micrograph (SEM) of the paramagnetic particles with magnification of 2.41×10^3. The magnetite crystal grains are dispersed in the central region of the latex spheres and appear as dark spots in the SEM.

IV. RESULTS AND DISCUSSION

Figure 2 shows the scanning electron micrograph (SEM) of the paramagnetic particles. The magnetite crystal grains are dispersed in the central region of the latex spheres and appear as dark spots in the SEM. It is seen from Fig. 2 that the particles have a wide size distribution. To prepare a dilute suspension of relatively uniform particles, we used a simple sedimentation method to separate the particles of different sizes. Because of the large density difference between the particles (2.24 g/cm^3) and water (1 g/cm^3), large particles will settle to the bottom of the sample cell in a day (under gravity). The sedimentation method used in the experiment is described as follows. First, a quantity of concentrated suspension was poured into a tall cylindrical cell. After several hours the top portion of the solution (typically 1/3) was pipetted out and put into another cylindrical cell. An aqueous solution of SDS (0.5 wt.%) was then added into the cell such that the total volume of the solution remains the same as before. This procedure could be repeated two or three times and the final suspension was found to be fairly monodispersed.

Figure 3 shows the measured scattering intensities $I_{A,Z}(q,0)$ and $I_{A,-Y}(q,0)$ as a function of the polarization angle A for different particles. All the measurements were carried out at the fixed scattering angle $\gamma=90°$. To have a meaningful comparison, three kinds of particles with different scattering properties were used in the experiment. The solid circles in Fig. 3(a) shows the measured $I_{A,Z}(q,0)$ for the polystyrene-butadiene latex spheres of diameter 0.21 μm. These particles are uniform nonmagnetic isotropic dielectric spheres with $\mu=0$ and $\beta=0$. It is seen that the measured $I_{A,Z}(q,0)$ (the AV scattering) for the isotropic dielectric particles can be well described by the function $I_{A,Z}(q,0)$

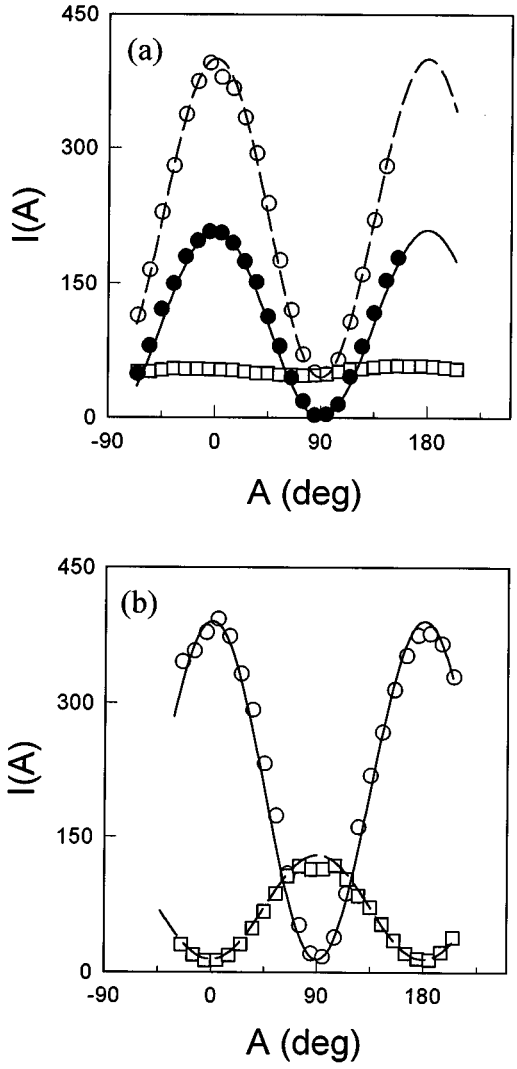

FIG. 3. Measured $I_{A,Z}(q,0)$ (solid and open circles) and $I_{A,-Y}(q,0)$ (open squares) as a function of the polarization angle A for the polystyrene-butadiene latex spheres [isotropic dielectric particles, solid circles in (a)], the PTFE particles [anisotropic dielectric rods, open symbols in (a)], and the paramagnetic particles [open symbols in (b)]. The solid and dashed curves are the fits to the data points (see text for details).

$=I_{VV}\cos^2 A$ (the solid curve) with $I_{VV}=210$ (arbitrary units). This function agrees well with Eq. (9) for the particles with $\mu=0$ and $\beta=0$. Because the dielectric particles scatter light isotropically, their AH scattering [i.e., $I_{A,-Y}(q,0)$]is found to be approximately zero for all values of A. [Due to the leakage of the analyzer, a small amount of light (less than 0.5% of the AV scattering) was detected in the AH scattering geometry.]

The open symbols in Fig. 3(a) represent the measured $I_{A,Z}(q,0)$ (circles) and $I_{A,-Y}(q,0)$ (squares) for the polytrafluoroethylene (PTFE) latex particles. The PTFE particles were synthesized by a dispersion polymerization process, which in the presence of the emulsifier yields stable aqueous latexes.[16] The latex particles thus formed possess a crystalline structure and optical anisotropy ($\beta\neq 0$).[17,18] Our recent light scattering measurements[19] revealed that the PTFE particles have a rod-like shape with an average length 0.45 μm and an average diameter 0.19 μm. As shown in Fig. 3(a), the AV scattering from the PTFE particles is well fitted by the function $I_{A,Z}(q,0)=I_{VV}\cos^2 A+I_{VH}$ (the dashed curve) with $I_{VV}=355$ and $I_{VH}=45$ (arbitrary units). The AH scattering, on the other hand, does not change with A and is the same as I_{VH}. These findings are in good agreement with the predictions of Eqs. (9) and (10) for the anisotropic dielectric particles with $\mu=0$ but $\beta\neq 0$. Note that for the PTFE particles the intensity ratio $I_{VH}/I_{VV}\simeq 13\%$, which is very large compared with other anisotropic dielectric particles.

Figure 3(b) shows the measured $I_{A,Z}(q,0)$ (circles) and $I_{A,-Y}(q,0)$ (squares) for the paramagnetic particles. The AV scattering of the paramagnetic particles is similar to that of the dielectric particles, and can be well fitted by the function $I_{A,Z}(q,0)=I_{VV}\cos^2 A+I_{VH}$ (the solid curve) with $I_{VV}=375$ and $I_{VH}=15$ (arbitrary units). However, the AH scattering of the paramagnetic particles differs greatly from that of the (anisotropic) dielectric particles, and goes as $I_{A,-Y}(q,0)=I_{HH}\sin^2 A+I_{VH}$ (the¬ dashed¬ curve) with $I_{HH}=115$ and $I_{VH}=15$ (arbitrary units). The two fitted functions agree well with Eqs. (9) and (10) for the (anisotropic) paramagnetic particles with $\beta\neq 0$ and $\mu\neq 0$. Figure 3 reveals that the anisotropy of the paramagnetic particles is weak because their intensity ratio I_{VH}/I_{VV} ($=4\%$) is approximately three times smaller than that of the PTFE particles. The magnetic dipole radiation contribution I_{HH}, however, is unusually large and equals to approximately 1/3 of the electric dipole radiation contribution I_{VV} ($I_{HH}/I_{VV}\simeq 31\%$). According to the theory of electrodynamics,[11] the intensity ratio I_{HH}/I_{VV} is usually proportional to $(a/\lambda_0)^2$, where a is a characteristic length of the effective magnetic dipole for the particles. Figure 3(b) thus suggests that the typical value of a for the paramagnetic particles is comparable with their radius ($\simeq 0.2$ μm). Because the magnetite grains dispersed inside a latex particle are very small, their magnetic energy (proportional to the volume of the grain) can be comparable with the thermal energy k_BT. Under this condition, the magnetization vector of each grain will become unstable and fluctuate in the same way as in a classical paramagnetic gas, except that the magnetic moment of the grains is much larger than that of paramagnetic atoms. This process is called superparamagnetism[20,21] and is presumably the reason why the latex particles, which contain many of these magnetite grains, possess no net magnetization in zero magnetic field at room temperature and can be easily magnetized by an external magnetic field without any hysteresis.[22] The data in Fig. 3(b) therefore indicates that the magnetic dipole radiation of the latex particles may be resulted from the alignment of the individual magnetite grains inside the particles. We notice that this alignment is induced by the incident laser light and the reason why these small magnetite grains can respond to the fast laser frequency needs to be further investigated.

We now discuss the measurements of the autocorrelation functions $I_{V,V}(q,t)$ and $I_{V,H}(q,t)$. In the experiment, the incident polarization direction $\mathbf{n}_i$ was set to be vertical (i.e., $A=0^0$), and the polarization direction $\mathbf{n}_f$ of the detected light was chosen to be either vertical (the VV scat-

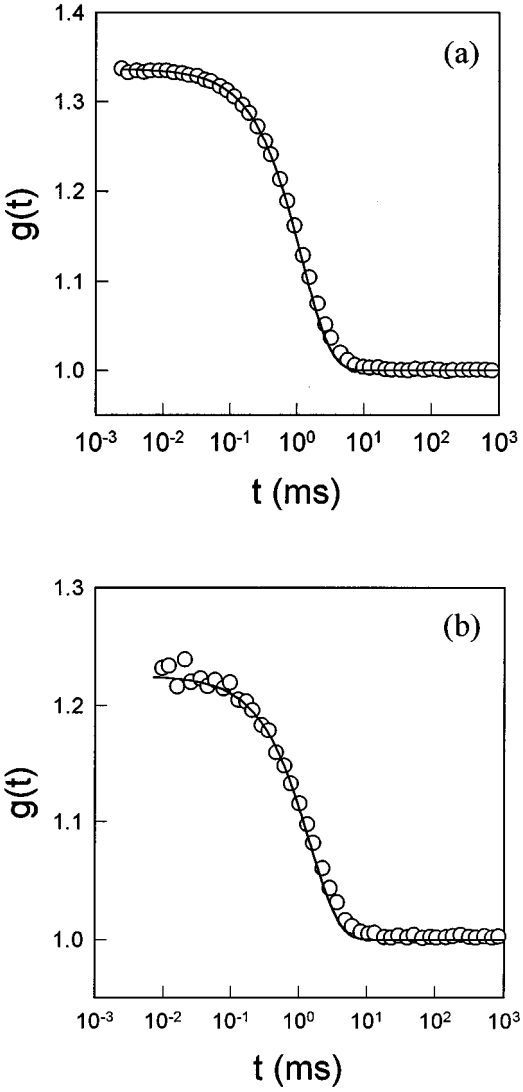

FIG. 4. Measured $g_{VV}(t)$ [circles in (a)] and $g_{VH}(t)$ [circles in (b)] as a function of the delay time t for the paramagnetic particles. The measurements were made at $\gamma=90°$. The solid curves are the fitted function $1+be^{-2\Gamma t}$.

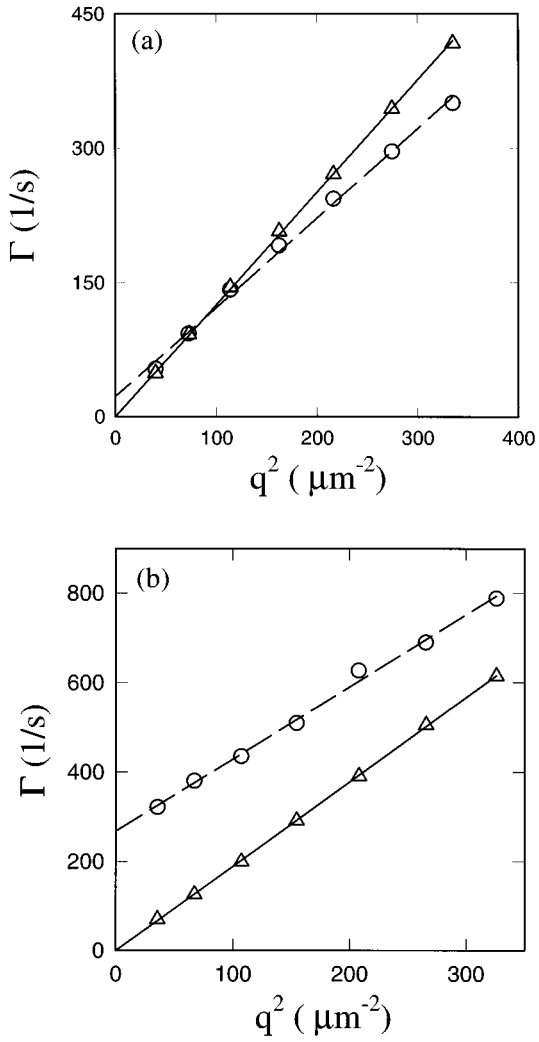

FIG. 5. Measured decay rate Γ as a function of q^2 in the *VH* (circles) and *VV* (triangles) scattering geometries. The solid and dashed lines are linear fits to the triangles and circles, respectively. The data in (a) were obtained from a polydispersed sample (no size selection) and those in (b) were obtained from a relatively monodispersed sample (with size selection).

tering) or horizontal (the *VH* scattering). Because the anisotropic scattering (proportional to β^2) of the paramagnetic particles is weak, the *VV* scattering is dominated by the isotropic scattering (proportional to α^2). Substituting Eq. (14) into Eq. (16), we have

$$g_{VV}(t)=1+b\left\{\frac{I_{V,V}(q,t)}{I_{V,V}(q,0)}\right\}^2\simeq 1+be^{-2Dq^2t}.\neg \qquad (17)$$

The *VH* scattering, on the other hand, is produced purely by the optical anisotropy of the particles. Substituting Eq. (15) into Eq. (16), we have

$$g_{VH}(t)=1+b\left\{\frac{I_{V,H}(q,t)}{I_{V,H}(q,0)}\right\}^2=1+be^{-2(6\Theta+Dq^2t)}.\neg \qquad (18)$$

Figure 4 shows the measured $g_{VV}(t)$ [Fig. 4(a)] and $g_{VH}(t)$ [Fig. 4(b)] as a function of the delay time t for the paramagnetic particles. The measurements were made at $\gamma=90°$. The solid curves are the fitted function $1+be^{-2\Gamma t}$ with $\Gamma=0.42$ ms^{-1}, $b=0.355$ for the *VV* scattering data [Fig. 4(a)] and $\Gamma=0.35$ ms^{-1}, $b=0.225$ for the *VH* scattering data [Fig. 4(b)]. It is seen that the simple exponential function fits the data well. Because the signal in the *VH* scattering geometry was weak, it took longer time to collect the data for $g_{VH}(t)$ with an adequate level of statistics when compared with the measurement of $g_{VV}(t)$. Note that the value of b (a measure of the signal-to-noise ratio) obtained in the *VH* scattering geometry is smaller than that in the *VV* scattering geometry.

According to Eqs. (17) and (18), the decay rate Γ in the *VH* scattering geometry is given by $\Gamma_{VH}=6\Theta+Dq^2$ and for the *VV* scattering $\Gamma_{VV}=Dq^2$. In the experiment, we measured Γ for different values of q by varying the scattering angle γ from 30° to 90°. Figure 5 shows the measured Γ as a function of q^2 in both the *VH* (circles) and *VV* (triangles) scattering geometries. The solid and dashed lines are the linear fits to the triangles and circles, respectively. The data in

TABLE I. Measured intensity ratio I_{VH}/I_{VV} for the paramagnetic particles with different radius R.

R (nm)	79¬	119¬	137¬	220
I_{VH}/I_{VV}(%)¬	0.37¬	1.6¬	2.5¬	5.75

Fig. 5(a) were obtained from a polydispersed sample, which was prepared by direct dilution of the stock solution without any size selection. The slope of the solid line in Fig. 5(a) gives the particle's diffusion constant $D=1.25\ \mu\text{m}^2/\text{s}$. Using Einstein's relation $D=k_BT/(6\pi\eta R)$, we get the particle radius $R=0.17\ \mu$m. Here k_BT is the thermal energy and η is the viscosity of the solvent. As one would expect, the intercept of the solid line is close to zero. It is seen from Fig. 5(a) that the dashed line has a slightly smaller slope than the solid line and the measured Γ_{VH} at large scattering angles becomes even smaller than Γ_{VV}. From the repeated measurements of Γ_{VV} and Γ_{VH} for the paramagnetic particles with different size distributions, we find that the measured Γ_{VH} is strongly influenced by the size polydispersity of the particles, whereas Γ_{VV} is robust and much less sensitive to the sample preparation procedures. To understand this effect, we measured the intensity ratio I_{VH}/I_{VV} for particles with different radius R. The size selection was carried out by the sedimentation method and the final results are listed in Table I. The measured I_{VH}/I_{VV} is found to increase linearly with R, suggesting that the large particles tend to have more magnetite content. This is because the anisotropic scattering (I_{VH}) is produced mainly by the tiny magnetite crystallites. Consequently, the larger particles weigh more in the *VH* scattering and therefore the average particle radius obtained from the *VH* scattering tends to be larger than that from the *VV* scattering. This explains why the slope of the measured Γ_{VH} is smaller than that of Γ_{VV}.

To have a scattering sample with relatively monodispersed particles, we used the sedimentation method to separate the particles of different sizes. The sample used in Fig. 5(b) was prepared by allowing the particle suspension in a tall cylindrical cell to settle for two days. After this period of time, most large particles have settled down to the bottom of the cell. The middle 1/3 of the solution was then pipetted out and put into the scattering cell. As shown in Fig. 5(b), the two fitted lines now have approximately the same slope, and the dashed line has a non-zero intercept. From the slope of the solid line we find $D=1.89\ \mu\text{m}^2/\text{s}$ and the corresponding $R=0.13\ \mu$m. The slope of the dashed line gives $D=1.61\ \mu\text{m}^2/\text{s}$ and the corresponding $R=0.15\ \mu$m. This value of R is close to but still 15% larger than the *VV* result. From the intercept of the dashed line we obtain $\Theta=44.6\ \text{s}^{-1}$. Using the equation $\Theta=k_BT/(8\pi\eta R^3)$ for the rotational diffusion constant of spherical particles,[12] we find the particle radius $R=0.15\ \mu$m which agrees with the value obtained from the slope. The above measurements suggest that the size distribution of the scattering sample used in Fig. 5(b) has been narrowed considerably, but it is still somewhat polydispersed. It should be mentioned that because the anisotropic scattering of the paramagnetic particles is rather weak, the measured Γ_{VH} is very sensitive to the leaking of the polarizers. When a small amount of the leaked *VV* scattering is mixed with the VH scattering, the measured intensity auto-correlation function $g(t)$ will become a sum of two exponential functions. If one still uses a single exponential function to fit the measured $g(t)$, the resulting decay rate Γ will be reduced to a value in between Γ_{VH} and Γ_{VV}.

V. CONCLUSION

We have studied light scattering properties of the polymer latex spheres which contain 67 wt.% magnetite (Fe_3O_4). The magnetite forms many tiny ferrimagnetic crystallites which are uniformly dispersed in the latex spheres. Because of the random orientation of the ferrimagnetic crystallites, these latex spheres possess no net magnetization in zero magnetic field. To account for the magnetic dipole radiation and the Brownian motion of the particles in a thermal equilibrium solution, we calculate the scattering intensity and its auto-correlation function $g(t)$ for different incident polarization direction $\mathbf{n}_i$ and different scattering angle γ. The calculation clearly delineates the difference in the scattering property between the dielectric and paramagnetic particles. Experimentally, we have examined the scattering properties of the paramagnetic particles and compare the results with those from isotropic and anisotropic dielectric particles. The experiment verifies the calculation and reveals that the magnetic dipole radiation of the paramagnetic particles is unusually large and equals to approximately 1/3 of the electric dipole radiation of the particles. The magnetic dipole radiation is presumably resulted from the alignment of the individual ferrimagnetic grains inside the particles, and that this alignment is induced by the incident laser light. Dynamic light scattering measurements show that the measured intensity auto-correlation function $g_{VH}(t)$ in the *VH* scattering geometry is strongly influenced by the size distribution of the particles, whereas $g_{VV}(t)$ in the *VV* scattering geometry is robust and much less sensitive to the sample preparation procedures. This is because the large paramagnetic particles tend to have more magnetite content and therefore weigh more in the depolarized *VH* scattering. With a simple sedimentation method, we were able to separate the particles of different sizes. The resulting suspension of the paramagnetic particles is found to be relatively monodispersed and gives the expected translational and rotational diffusion constants of the particles.

ACKNOWLEDGMENTS

We thank Christopher M. Sorensen and Xiaolun Wu for useful discussions. This work was supported by the National Science Foundation under Grant No. DMR-9623612.

[1] H. Wang *et al.*, Phys. Rev. Lett. **72**, 1929 (1994).
[2] J. Liu *et al.*, Phys. Rev. Lett. **74**, 2828 (1995).
[3] E. Lemaire *et al.*, J. Rheol. **39**, 1011 (1995).
[4] J. -C. Bacri *et al.*, J. Colloid Interface Sci. **132**, 43 (1989).
[5] M. Mohebi, N. Jamasbi, and J. Liu, Phys. Rev. E, **54**, 5407 (1996).

[6] Y. H. Hwang and X.-l. Wu, Phys. Rev. E, **49**, 3102 (1994); Phys. Rev. Lett. **74**, 2284 (1995).
[7] Information Manual, *Uniform Latex Particles* (Seradyn, Inc., Indianapolis, IN, 1987).
[8] J.-C. Bacri *et al.*, J. Phys. (Paris) **48**, 1385 (1987).
[9] D. Sohn, L. M. DeLong, and P. S. Russo, Mater Res. Soc. Symp. Proc. **248**, 247 (1992).
[10] M. Y. Lin, W. Luo, and J. Lynn, Mater Res. Soc. Symp. Proc. **375**, 341 (1995).
[11] See, e.g., J. D. Jackson, *Classical Electrodynamics*, 2nd ed. (Wiley, New York, 1975).
[12] B. J. Berne and R. Pecora, *Dynamic Light Scattering* (Wiley, New York, 1976).
[13] See, e.g., *Photon Correlation Spectroscopy and Velocimetry*, edited by H. Z. Cummins and E. R. Pike (Plenum, New York, 1977).
[14] R. Piazza, V. Degiorgio, M. Corti, and J. Stavans, Phys. Rev. B **42**, 4885 (1990).
[15] R. Piazza and V. Degiorgio, Phys. Rev. Lett. **67**, 3868 (1991).
[16] R. H. Ottewill and D. G. Rance, Colloid Polym. Sci. **264**, 982 (1986).
[17] T. Bellini, R. Piazza, C. Sozzi, and V. Degiorgio, Europhys. Lett. **7**, 561 (1988).
[18] R. Piazza, J. Stavans, T. Bellini, and V. Degiorgio, Opt. Commun. **73**, 263 (1989).
[19] P. Tong, K.-Q. Xia, and B. J. Ackerson, J. Chem. Phys. **98**, 9256 (1993).
[20] J. Crangle, *Solid State Magnetism* (Van Nostrand Reinhold, New York, 1991).
[21] A. H. Morrish, *The Physical Principles of Magnetism* (Wiley, New York, 1965).
[22] J. Ugelstad *et al.*, in Proceedings of the International Workshop in Polymer Reaction Engineering, Berlin, 1986 (unpublished).